Correspondence

Comments on "The Effect of the Imperfect Realization of the Artificial Mains Network Impedance on the Reproducibility of Conducted Emission Measurements"

Frédéric Broydé, *Senior Member, IEEE*,
and Evelyne Clavelier, *Senior Member, IEEE*

***Abstract*—This correspondence presents the relationship between impedance tolerance circles and the input impedance domains (IIDs) introduced and investigated some years ago. We also show the relevance of IID assessment to select an AMN.**

***Index Terms*—Artificial mains network (AMN), conducted emission, input impedance domain, power-line filter.**

I. Introduction

The impedance presented by an artificial mains network (AMN) to an equipment under test (EUT) has an influence on conducted emission measurements results. A recent paper [1] provides a detailed analysis of the deviation in measured emission levels caused by a deviation of the actual AMN impedance (seen by the EUT) from the corresponding impedance presented by the ideal AMN specified in a standard [2]. This analysis is based on the concept of impedance tolerance circle, defined as the boundary of a disk which must contain the impedance seen by the EUT, in line with the definition used in [3].

This correspondence shows that impedance tolerance circles are related to the concept of input impedance domain (IID) of a power-line filter, which was introduced and applied to AMNs more than 20 years before [3] was published. We provide corrections to earlier results on IIDs, and show that IIDs computed for an AMN may indicate that it is unsuitable for conducted emission measurements.

II. Input Impedance Domain

The input impedance, denoted by Z'_L, of a two-port linear filter depends on the impedance seen by the output port, that is the load impedance, denoted by Z_L. At any given frequency, the IID of the filter, denoted by D, is defined as the set of the input impedance values obtained when Z_L traverses the half complex plane, denoted by $\mathbb{C}_+$, of the complex numbers having a non-negative real part, so that we may write

$$D = \{Z'_L(Z_L) | Z_L \in \mathbb{C}_+\} \tag{1}$$

where the notation $Z'_L(Z_L)$ indicates that, in (1), Z'_L is regarded as a function of Z_L. This definition, mentioned in [4], seems to have been first introduced in [5] and [6], where the following results were stated.

1) D is either the half plane $\mathbb{C}_+$, or a half-plane of equation $\mathrm{Re}(z) \geq k$, where Re denotes the real part and k is a positive real number, or a disk contained in $\mathbb{C}_+$.
2) D is equal to $\mathbb{C}_+$ when the filter is lossless.

Manuscript received February 13, 2013; revised March 9, 2013; accepted March 18, 2013. Date of publication April 15, 2013; date of current version December 10, 2013.

The authors are with Excem, 78580 Maule, France (e-mail: fredbroyde@eurexcem.com; eclavelier@eurexcem.com).

Color versions of one or more of the figures in this paper are available online at http://ieeexplore.ieee.org.

Digital Object Identifier 10.1109/TEMC.2013.2256140

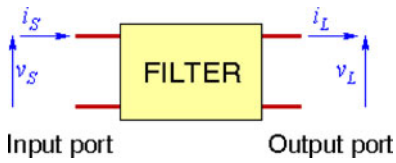

Fig. 1. Two-port filter.

More precisely, let us consider the two-port linear filter shown in Fig. 1, characterized by a chain matrix denoted by **A** and defined by

$$\begin{pmatrix} v_L \\ i_L \end{pmatrix} = \mathbf{A} \begin{pmatrix} v_S \\ i_S \end{pmatrix} = \begin{pmatrix} a_{11} & a_{12} \\ a_{21} & a_{22} \end{pmatrix} \begin{pmatrix} v_S \\ i_S \end{pmatrix}. \tag{2}$$

Let us use b_{ij} and c_{ij} to denote the real part and the imaginary part of a_{ij}, respectively. Assuming a passive and reciprocal filter, we can say that

a) if $a_{21} = 0$, then D is the half-plane defined by the inequation

$$\mathrm{Re}(z) \geq -\frac{b_{12}}{b_{11}} \quad \text{where} \quad -\frac{b_{12}}{b_{11}} \geq 0 \tag{3}$$

b) if $a_{21} \neq 0$ and $a_{11} = 0$, then D is the half-plane defined by the inequation

$$\mathrm{Re}(z) \geq -\frac{c_{22}}{c_{21}} \quad \text{where} \quad -\frac{c_{22}}{c_{21}} \geq 0 \tag{4}$$

c) if $a_{21} \neq 0$ and $a_{11} \neq 0$, then we can define θ and φ such that

$$\theta \in [0,\, 2\pi[\quad \text{and} \quad -a_{21}^2 = \left|a_{21}^2\right| e^{j\theta} \tag{5}$$

$$\varphi \in \left[-\frac{\pi}{2}, \frac{\pi}{2}\right] \quad \text{and} \quad -\frac{a_{11}}{a_{21}} = \left|\frac{a_{11}}{a_{21}}\right| e^{j\varphi}. \tag{6}$$

In the last case (c), D is either the half-plane defined by (3) if $\varphi = \pm\pi/2$, or a disk of center C and radius ρ if $\varphi \neq \pm\pi/2$, C and ρ being given by

$$C = \frac{e^{-j\theta}}{2\left|a_{11}a_{21}\cos\varphi\right|} - \frac{a_{22}}{a_{21}} \tag{7}$$

and

$$\rho = \frac{1}{2\left|a_{11}a_{21}\cos\varphi\right|}. \tag{8}$$

Here, we have presented the result in the form used in [5] and [6], with a correction of the sign in (6). However, another form is possible for the last case: if $a_{21} \neq 0$ and $a_{11} \neq 0$, D is either the half-plane defined by (3) if $\mathrm{Re}(a_{11}/a_{21}) = 0$, or a disk of center C and radius ρ if $\mathrm{Re}(a_{11}/a_{21}) \neq 0$, C and ρ being given by

$$C = \frac{1}{2a_{21}^2\,\mathrm{Re}\left(\frac{a_{11}}{a_{21}}\right)} - \frac{a_{22}}{a_{21}} \tag{9}$$

and

$$\rho = \frac{-1}{2\left|a_{21}^2\right|\mathrm{Re}\left(\frac{a_{11}}{a_{21}}\right)}. \tag{10}$$

This form is more compact, but it hides the fact that our proof of this result uses a geometric approach involving line inversion and rotations.

In the case of a lossless filter, it can be shown that $b_{12} = b_{21} = c_{11} = c_{22} = 0$. Consequently, in this case, $D = \mathbb{C}_+$. We see that losses are necessary to obtain an IID of finite radius.

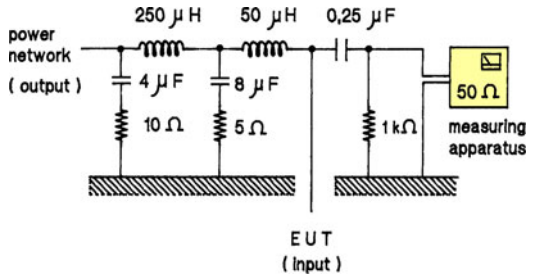

Fig. 2. First AMN considered in Section II.

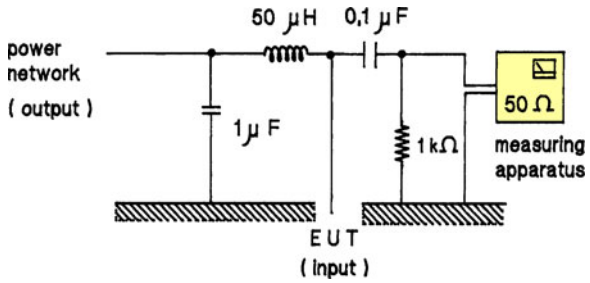

Fig. 3. Second AMN considered in Section II.

III. Application to Artificial Mains Networks

IIDs were introduced to analyze the performance of power-line filters, but the concept is also applicable to AMNs. For an AMN, if we assume that the uncertainty in the impedance seen by the EUT is only caused by the effect of the unknown impedance of the power network, the impedance tolerance circle (at a given frequency) is the boundary of the IID (at this given frequency).

The IIDs of two different AMNs were investigated in [7, Sec. III]. Since the numerical results and plots on IIDs contained errors in [7], we shall revisit this question and consider the first AMN of Fig. 2 and the second AMN of Fig. 3, which are the "50 Ω/50 μH + 5 Ω V-network" and the "50 Ω/50 μH V-network" defined in [2, Annex A], respectively. Assuming ideal circuit elements, their IIDs can be computed using the theory of Section II. As an example, boundaries of the IIDs obtained at five frequencies with the first AMN are shown in Fig. 4. We shall also consider a third AMN, which is identical to the second AMN, except that the 1 μF capacitor, instead of being an ideal circuit element, has an equivalent series resistance of 10 $\mu\Omega$.

In the case of an AMN connected to a mains outlet of unknown impedance, the radius of the IID is a measure of the uncertainty in the impedance seen by the EUT. We have plotted in Fig. 5, the radius of the IID of the first, second, and third AMNs versus frequency. We see that the radius of the IID is less than 1 Ω at frequencies higher than about 8 kHz in the case of the first AMN, and at frequencies higher than about 2.3 MHz in the case of the third AMN. At frequencies below 2 MHz, the losses in the third AMN are insufficient to guarantee a small IID radius. Having less losses, the second AMN is such that the radius of its IID is greater than about 24 Ω at any frequency.

On this basis, it is possible to conclude that the second and third AMNs seem inadequate for measurement in the frequency range 150 kHz to 30 MHz, in an implementation where the impedance of the mains is not controlled. Losses in the coil and capacitors of an actual AMN built according to the schematic diagram of Fig. 3 will reduce the radius of the IID, as evidenced by a comparison between the second and third AMNs. Such losses are therefore desirable, up to a certain point, even though they are not specified in [2, Annex A].

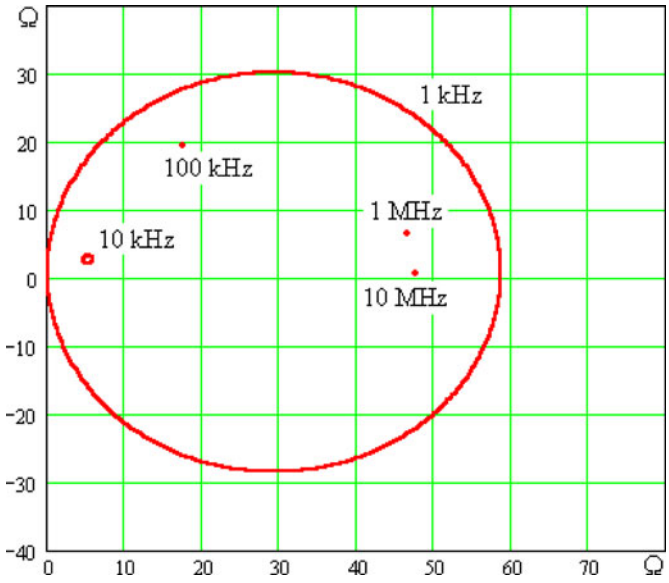

Fig. 4. Boundaries of the IIDs of the first AMN at five frequencies.

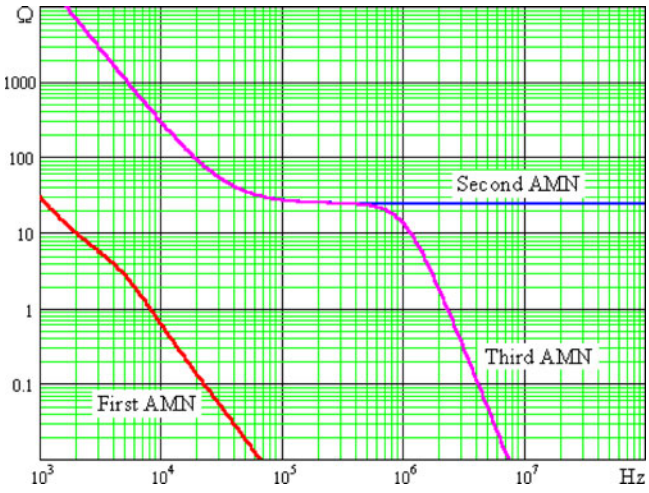

Fig. 5. Radius of the three AMNs versus frequency.

References

[1] C. F. M. Carobbi and M. Stecher, "The effect of the imperfect realization of the artificial mains network impedance on the reproducibility of conducted emission measurements," *IEEE Trans. Electromagn. Compat.*, vol. 54, no. 5, pp. 986–987, Oct. 2012.

[2] *Specification for Radio Disturbance and Immunity Measuring Apparatus and Methods — Part 1-2: Radio Disturbance and Immunity Measuring Apparatus — Ancillary equipments — Conducted Disturbances*, Edition 1.2, International Electrotechnical Commission, CISPR 16-1-2, 2006.

[3] *Specification for Radio Disturbance and Immunity Measuring Apparatus and Methods — Part 4-2: Uncertainties, Statistics and Limits Modelling — Measurement Instrumentation Uncertainty*, Edition 2.0, International Electrotechnical Commission, CISPR 16-4-2, 2011.

[4] F. Broydé and E. Clavelier, "Some issues on the characterization of power-line filters and related standards," *IEEE Trans. Electromagn. Compat.*, vol. 51, no. 3, pp. 876–877, Aug. 2009.

[5] F. Broydé and E. Clavelier, "Minimum attenuation and input impedance domain of a linear filter," in *Proc. 8th Int. Zürich Symp. Electromagn. Compat.*, Mar. 1989, pp. 261–266.

[6] F. Broydé and E. Clavelier, "Atténuation minimale et domaine d'impédance d'entrée d'un filtre linéaire," in *Proc. 5ème Colloque Int. sur la CEM*, Sep. 12–14, 1989, Paper BII-3.

[7] F. Broydé and E. Clavelier, "Designing power-line filters for their worst-case behaviour," in *Proc. 9th Int. Zürich Symp. Electromagn. Compat.*, Mar. 1991, pp. 583–588.